Nanocrystalline titanium dioxide prepared by hydrothermal method and its application in dye-sensitised solar cells

Qiaolin Han[1], Min Yu[1], Jiang Liu[1,2,3]

[1]*School of Chemistry and Chemical Engineering, South China University of Technology, Guangzhou 510641, People's Republic of China*
[2]*The Key Laboratory of Fuel Cell Technology of Guangdong Province, Guangzhou 510641, People's Republic of China*
[3]*The Key Laboratory of Enhanced Heat Transfer and Energy Conservation, Ministry of Education, Guangzhou 510641, People's Republic of China*
E-mail: jiangliu@scut.edu.cn

Published in Micro & Nano Letters; Received on 10th December 2012; Accepted on 8th March 2013

Nanocrystalline TiO_2 was prepared through hydrothermal synthesis using tetrabutyl titanate as starting material. With a constant reaction time of 12 h, the reaction temperature was changed from 120 to 160°C and the pH value of the reaction medium was ranged from 1 to 9. Every specimen of the as-prepared TiO_2 powder was characterised by X-ray diffraction, a scanning electron microscope, transmission electron microscopy, high-resolution transmission electron microscopy, selected area electron diffraction and was also used to fabricate dye sensitised solar cells (DSSCs). The experimental results showed that the phase of the powder was affected by the pH value, whereas the particle size depended on the reaction temperature. Pure anatase TiO_2 was obtained with the pH value of 3. The solar energy conversion efficiency (η) of the DSSC fabricated with the pure anatase TiO_2 prepared at 140°C was 3.64%, which was higher than those with the TiO_2 prepared under any other conditions. The purchased TiO_2 (P25) was used to make a DSSC for comparison. It turned out that the performance of all the DSSCs with TiO_2 prepared by hydrothermal synthesis was higher than that with the P25.

1. Introduction: Being the most promising substitution for traditional silicon solar cells, dye-sensitised solar cells (DSSCs), whose photo-electrical energy conversion efficiency has already reached 12% [1], have attracted widespread academic and industrial interest. A DSSC consists of sensitising dye, transparent conducting substrates, nanocrystalline TiO_2 thin film, I^-/I_3^- redox electrolyte and a Pt counter electrode, among which, the film of TiO_2 with nanocrystalline morphology, as the photoanode, plays a very important role in photon absorption, electron transportation and electron collection. Because of different sequence of [TiO_6] octahedron, TiO_2 may form three homogeneous isomer phases – anatase, rutile and brookite. Rutile is the most thermodynamically stable phase possessing a smaller bandgap energy (3.0 eV) than that of the anatase phase (3.2 eV), but anatase performs a higher photocatalytic activity [2].

Many different methods have been reported to synthesise TiO_2 nanoparticles, such as the sol–gel method [3–5], the solvothermal method [6–9], the hydrolysis method and so on. Among which, hydrothermal synthesis has the advantages of providing monodispersed particles, controlled particle morphology and phase homogeneity [10]. In hydrothermal synthesis, a Teflon-lined stainless-steel autoclave is used as the reactor. An aqueous environment with high pressure can be established within the reactor when a closed autoclave is heated to a certain temperature, and some generally insoluble substances can be dissolved in the aqueous medium. Recrystallisation occurs during the autoclave cooling down [10], then highly crystalline products can be obtained at relatively low temperatures.

A variety of mixtures of anatase, rutile and brookite of TiO_2 have been produced by hydrothermal synthesis under different conditions. TiO_2 nanopowders with different anatase/rutile ratios were obtained using tetrabutyl titanate $Ti(OC_4H_9)_4$ (TTBT) as a precursor, with acid aqueous media such as HCl, HNO_3, H_2SO_4 and CH_3COOH, at different temperatures [11–13]. Wang and co-workers used TTBT to prepare mesoporous nanocrystalline TiO_2 powders at 150–200°C, the photocatalytic activity of which greatly exceeded that of Degussa P25 [13]. Pavasupree *et al.* synthesised anatase TiO_2 nanopowder using TTBT, by keeping the reaction temperature at 130°C for 12 h and the photoconversion efficiency of the anatase TiO_2-based cell was about 6.30%, higher than 5.82% of P25 [14]. Pure rutile titania nanocrystallites were synthesised using $TiCl_4$ as starting material and several kinds of acids as reaction media [2, 9, 15–18]. A mixture of anatase, brookite and rutile TiO_2 nanocrystallites was obtained by hydrothermal treatment using titanium (IV) isopropoxide as starting material [19, 20]. Anatase or rutile nanoparticles were synthesised by hydrothermal treating tetra-alkyl ammonium hydroxides (TANOH) at 240°C [21–23]. These studies showed that in hydrothermal synthesis, the reaction temperature and the pH value of the medium play important roles in the phase composition of the products. However, the effects of reaction temperature and pH value of the reaction medium on the properties of the products have seldom been investigated systematically.

Herein, we report our research on synthesising nanocrystalline TiO_2 by the hydrothermal method, with TTBT as the titanium source. A series of medium pH values (1, 3, 5, 7 and 9) are, respectively, applied by controlling the concentration of the medium (HCl or NaOH) solutions. The series syntheses are also carried at different temperatures. The obtained TiO_2 powders are characterised by X-ray diffraction (XRD) to determine the optimised condition for synthesising anatase TiO_2, whose high photocatalytic activity is favoured for DSSC application. The details of particle size, microstructure and the extent of agglomeration are also examined through a scanning electron microscope (SEM) and transmission electron microscopy (TEM). The performance of photo-electrical conversion efficiency is demonstrated by testing DSSCs prepared with the synthesised TiO_2.

2. Experimental

2.1. Preparation of TiO_2 nanocrystals: Five media with pH values of 1, 3, 5, 7 and 9, respectively, were prepared by dissolving a proper amount of HCl (Guangdong, AR) or NaOH (Guangdong, AR) in distilled water. TTBT (9.5 ml) was added drop-wise to 45 ml of each of the mediums under vigorously stirring. Immediately, a large amount of white precipitate appeared. The TTBT-added medium had been continuously stirred for 4 hours

doi: 10.1049/mnl.2012.0941

before it was transferred into a Teflon-lined stainless-steel autoclave (60–80% filled) and heat treated at a certain reaction temperature for 12 h. Reaction temperatures of 120, 140 and 160°C were, respectively, selected for the experiments. After the hydrothermo reaction, the autoclave was cooled down naturally in air. Subsequently, the white precipitate was separated by centrifugation and then washed with ethanol until the liquid became neutral. The product was dried at room temperature overnight and ground into a fine powder. Finally, it was calcined at 500°C for 3 h.

2.2. DSSC fabrication and measurement: A schematic illustration of the structure of a DSSC, consisting of a photoanode, counter electrode and electrolyte [24], and its performance testing set is shown in Fig. 1.

The photoanode is a thin layer of dye-sensitised mesoporous TiO_2 nanocrystalline film coated on a conductive glass. The as-prepared TiO_2 powders and the purchased TiO_2 powder (P25, Degussa, Germany) were used to fabricate thin films for DSSCs. In a weight ratio of 1:6:0.8, TiO_2 powder, terpineol and polyvinyl butyral (PVB) were mixed by ball-milling to form a well-dispersed slurry. A piece of indium-doped tin oxide (ITO) conductive glass (10 Ω/cm^2, $d = 1.1$ mm; Shenzhen, China) (5 × 2 cm) was used as the substrate. A 4–5 mm strip was masked using Scotch tape (3 M) at each of the two longer edges of the conducting side of the ITO glass. Then a layer of TiO_2 film was deposited on the exposed area using the TiO_2 slurry with the doctor blade method [14, 25]. After being sintered at 450°C for 30 min, the ITO glass was cut to obtain three smaller equal-area (∼1.6 × 2 cm) pieces. A wooden toothstick was used to carefully scrape the four edges of the TiO_2 film on each piece to obtain an even and smooth film with an effective area of 0.5 × 0.5 cm The as-prepared film was immersed in an ethanol solution containing ruthenium (II) dye (known as N719, 0.5×10^{-3} mol/l; Solarnix, Switzerland) overnight. Then it was washed and dried at room temperature.

The counter electrode was prepared by coating a thin layer of Pt layer (thickness, 300 nm) on an ITO glass (∼ 1.6 × 2 cm) with the RF magnetron sputtering method. The Pt layer serves as a catalyst for the triiodide-to-iodide regeneration reaction of the electrolyte.

For the iodide–triiodide electrolyte, four solutions, LiI (0.2 mol/l), I_2 (0.1 mol/l), 1,2-dimethyl-3-propylimidazolium iodide (DMPII) (0.6 mol/l) and 4-tert-Butyl Pyridine(4-tBP) (0.5 mol/l), all with 3-methoxypropionitrile as solvent, were separately prepared first. Then the four solutions were mixed in a volume ratio of 1:1:0.5:0.5.

The as-prepared photoanode and the Pt-coated counter electrode were oppositely overlapped in a way that the TiO_2 film was faced to and covered by the Pt layer of the counter electrolyte, with some of the photoanode edge area not coated by TiO_2 exposed (Fig. 1). Two binder clips were used to hold the plates together. Then the redox electrolyte was injected into the interspace between them using a syringe.

The completed DSSC was tested under illumination of a solar simulator whose light intensity was adjusted to AM-1.5 radiation with an Si solar cell (Oriel M-95510, USA). The photocurrent–voltage curves were measured with a digital source meter (Keithley model 2400, USA).

2.3. Property characterisation of materials: The crystal-phase was characterised by an X-ray diffractometer (XRD, Bruker D8advance, Germany) over a 2θ range from 10° to 80° using Cu Kα ($\lambda = 0.15406$ nm) radiation at 40 kV and 40 mA. The scanning step was 0.02°/min. The morphology and the dispersion of particles were investigated by TEM (JEOL JEM-2100HR, Japan), high-resolution transmission electron microscopy (HRTEM, equipment in TEM) and the lattice fringes were measured by selected area electron diffraction (SAED, equipment in TEM). The samples for TEM were prepared by dispersing the corresponding powders in ethanol under ultrasonic, then dropping the suspension onto a copper grid. The crystal microstructure and surface morphology of the synthesised TiO_2 powder and TiO_2 thin films were examined by SEM (Philips XL-30FEG, Holland).

3. Results and discussion

3.1. XRD characterisation of the TiO_2 powders: Fig. 2 shows the XRD spectra of the products synthesised at 160°C under a variety of pH values of the media, along with that of the commercial P25 as comparison. It can be seen that when the pH value of the medium is 1, the main phase of the synthesised TiO_2 is anatase, with a small fraction of rutile and brookite. The phase of the powder synthesised under the medium pH of 3 is pure anatase. All the products obtained under larger pH values are anatase with a trace of brookite. A similar situation is observed for the powders synthesised at 120 and 140°C. However, the commercial TiO_2 (P25) is a mixture of anatase and rutile, with a much higher relative intensity of rutile than that of all the specimens prepared by hydrothermal synthesis.

Based on the XRD spectra of the TiO_2 nanocrystals, the proportion of each of the three phases in a sample can be calculated by (1)–(3) [26–28]

$$W_A = k_A A_A / (k_A A_A + A_R + k_B A_B) \quad (1)$$

$$W_R = A_R / (k_A A_A + A_R + k_B A_B) \quad (2)$$

$$W_B = k_B A_B / (k_A A_A + A_R + k_B A_B) \quad (3)$$

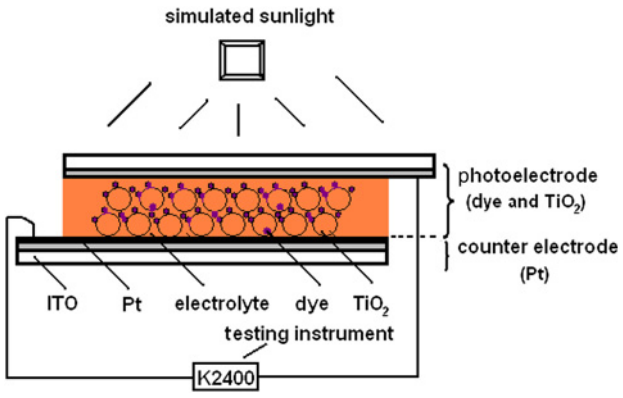

Figure 1 *Structure of DSSCs*

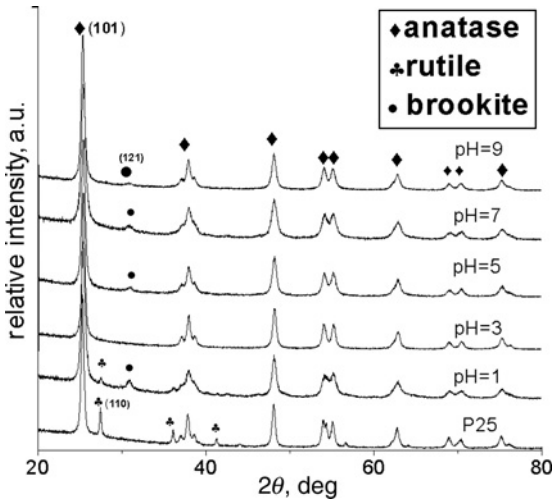

Figure 2 *XRD patterns of hydrothermal synthesised TiO_2 nanocrystals obtained at constant reaction time of 12 h for different pH at 160°C*

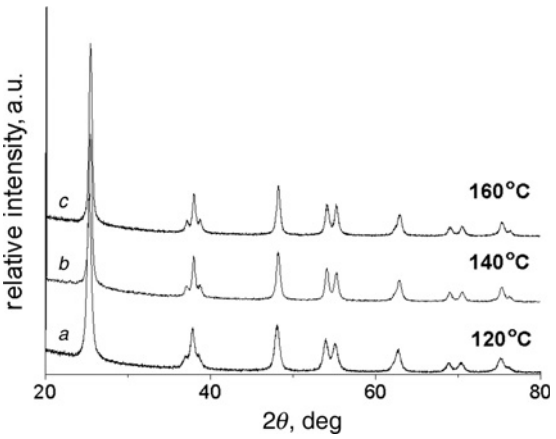

Figure 3 *XRD patterns of hydrothermal synthesised TiO_2 nanocrystals obtained at a constant pH of 3 from different reaction temperatures*
a 120°C
b 140°C
c 160°C

where W_A, W_R and W_B represent the weight fractions of the anatase, rutile and brookite phases, respectively. A_A, A_R, A_B are the integrated intensities of the anatase (101), rutile (110) and brookite (121) peaks, respectively. The coefficients k_A and k_B are coefficients with values of 0.886 and 2.721, respectively. Using the data of Fig. 2, the weight fraction of anatase of the TiO_2 synthesised under pH values of 1, 3, 5, 7 and 9 is calculated as 81, 100, 89, 87 and 85%, respectively. It can be seen that the anatase proportion depends on the pH value of the medium in a way of monotone function, which is an increasing function when pH < 3 and is a decreasing one when pH > 3. At pH = 3, the synthesised TiO_2 is pure anatase. The commercial P25 is a mixture of anatase and rutile whose fractions are calculated to be 75 and 25%, respectively. It is obvious that the anatase fraction of all the synthesised TiO_2 is larger than that of the commercial P25.

Fig. 3 shows the XRD patterns of the TiO_2 powders synthesised at different temperatures under the medium pH of 3. They are all pure anatase. The average crystal particle size calculated by Scherrer's equation are 17.1, 18.3 and 20.4 nm for the powders synthesised at 120, 140 and 160°C, respectively. It turns out that the particle size of the TiO_2 increases with synthesising temperature.

3.2. Morphology characterisation: Fig. 4 illustrates the SEM and TEM images of the TiO_2 powders synthesised at 120°C (*a*, *b*), 140°C (*c*, *d*) and 160°C (*e*, *f*), respectively, under the medium pH value of 3 and also shows the HRTEM image and SAD pattern (*i*) of sample at 140°C under pH of 3. The images of the commercial P25 (*g*, *h*) are also shown as comparison. It can be seen that the particles of all the powders are spherical, with a narrow particle size distribution. The average particle size is consistent with that estimated with the XRD analysis (~20 nm). While the particles of the commercial P25 are well dispersed (Figs. 4*g* and *h*), agglomeration is observed in the SEM images of the TiO_2 powders by hydrothermal synthesis (Figs. 4*a*, *c* and *e*). However, this agglomeration belongs to soft reunion and can be separated by dispersant and mechanical force (e.g. supersonic treatment or grinding) as shown in the TEM images (Figs. 4*b*, *d* and *f*). The HRTEM image (Fig. 4*i*) of the pure-anatase TiO_2 synthesised at 140°C under pH of 3 shows the lattice fringes. The distance between the two adjacent lattice planes is 0.35 nm, which matches the value of (101) crystallographic plane of anatase TiO_2. The SAED pattern (inset of Fig. 4*i*) illustrates some amorphous TiO_2 exists, which is corresponding to the crystallinity of the XRD pattern and the crystallographic rings corresponding to the anatase phase.

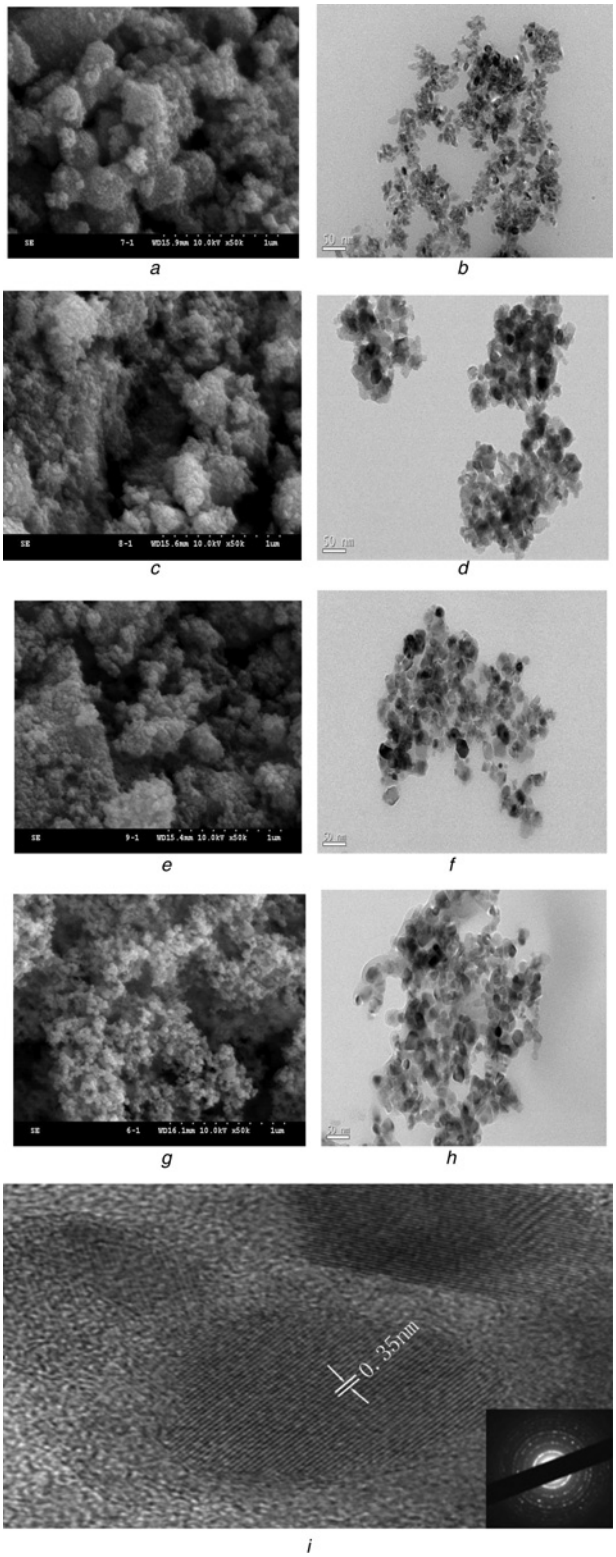

Figure 4 *SEM and TEM micrographs hydrothermal synthesised TiO_2 nanocrystals under pH of 3 from different temperatures*
a and *b* 120°C
c and *d* 140°C
e and *f* 160°C
g and *h* Commercial P25
i HRTEM image and SAD pattern of sample at 140°C under pH of 3

Fig. 5 shows the surface (*a*) and cross-sectional (*b*) SEM micrographs of the TiO_2 film prepared with the TiO_2 nanopowder synthetised under pH of 3. From Fig. 5*a*, the agglomeration of the surface

doi: 10.1049/mnl.2012.0941

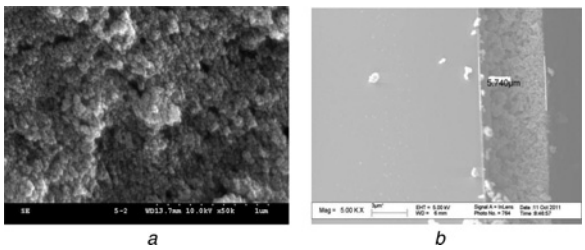

Figure 5 *SEM micrographs of TiO_2 film synthesised under pH of 3*
a Surface
b Cross-sectional

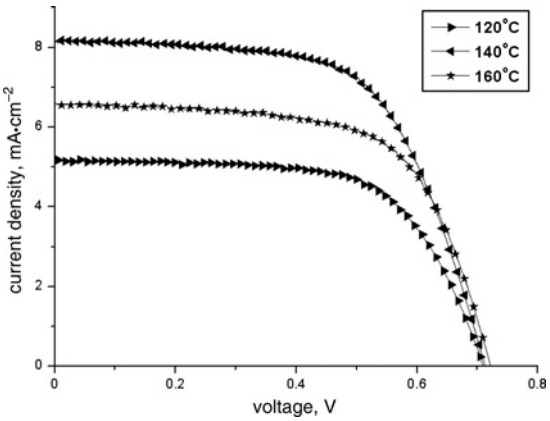

Figure 6 *Performance comparison of the I–V characteristics of DSSC assembled with the as-synthesised TiO_2 of pH = 3 at different temperatures*

can be seen, but this agglomeration is fluffy and it would be improved by adding some surfactant. Fig. 5*b* shows that the thickness of the TiO_2 thin film is 5.74 μm and it is in good contact with the ITO conductive surface.

3.3. Performance comparison of DSSCs: As anatase performs the highest photocatalytic activity among the three forms of TiO_2 and pure anatase has been obtained by hydrothermal synthesis under the medium pH value of 3, the TiO_2 powders synthesised under pH of 3 were firstly selected to fabricate the TiO_2 films for DSSCs. Fig. 6 shows the *I–V* characteristics of the DSSCs fabricated with TiO_2 synthesised at 120, 140 and 160°C, respectively. As shown in Fig. 6, the open circuit voltages of the three DSSCs are almost the same, about 0.71 V. The short-circuit current densities for the DSSCs corresponding to the TiO_2 synthesising temperatures of 120, 140 and 160°C are 5.15, 8.17 and 6.63 mA/cm^2, respectively.

The photo-to-electric energy conversion efficiency is calculated according to (4)

$$\eta = V_{oc} I_{sc} ff / P_{in} \times 100 \quad (4)$$

where η is the overall conversion efficiency, V_{oc}, I_{sc} and *ff* are the open-circuit voltage, short-circuit current density and fill factor, respectively. P_{in} is the intensity of the incident light (100 mW/cm^2). Based on the above data, the corresponding photo-to-electric energy conversion efficiencies of the three DSSCs are 2.37, 3.64 and 3.06%, respectively, by calculation, all of these are higher than the reported energy conversion efficiencies 0.25% [29] and 1.36% [30], although they are lower than some others (e.g. 4.3% [13] and 7.1% [25]).The DSSC with the TiO_2 synthesised at the reaction temperature of 140°C performs the best. As mentioned above, the particle size of the synthesised powder increases with

Table 1 Performance comparison of DSSCs assembled TiO_2 prepared with reaction temperature of 140°C under different pH values

Samples	Anatase content, %	Voc, V	I_{sc}, mA/cm^2	FF	η, %
pH = 1	81	0.71	4.62	0.66	2.17
pH = 3	100	0.71	8.17	0.62	3.64
pH = 5	89	0.68	7.20	0.62	3.02
pH = 7	87	0.69	7.33	0.66	3.31
pH = 9	85	0.72	6.44	0.64	2.98
P25	75	0.68	5.65	0.55	2.12

reaction temperature, resulting in the largest particle size of the powder synthesised at 160°C and the smallest size of that at 120°C. Generally, smaller particles will give a larger specific area that can provide more active sites for photo absorption and reaction in a DSSC, leading to higher output and photo-to-electric energy conversion efficiency. However, small particles tend to agglomerate together so that the practical specific area is reduced. It is obvious that among the three TiO_2 powders used to prepare DSSCs, the optimised is the one synthesised at 140°C.

Table 1 shows the performance comparison of DSSCs based on the TiO_2 powders synthesised at 140°C under different medium pH values. It can be seen that the short-circuit current (I_{sc}) and the conversion efficiency of the DSSCs have close corresponding relations to the anatase fraction in TiO_2. Under pH value of 3, the phase is pure anatase and the corresponding DSSC has both the highest I_{sc} (8.17 mA/cm^2) and the highest photo-to-electric energy conversion efficiency (3.64%), Meanwhile, the DSSC prepared with P25 which has the lowest anatase fraction, gives the lowest I_{sc} and conversion efficiency. The performance of all the TiO_2 prepared by hydrothermal synthesis is higher than that of the purchased P25.

4. Conclusions: TiO_2 nanocrystals have been synthesised via hydrothermal synthesis using TTBT as the titanium source. The effects of medium pH value and reaction temperature on the properties of products were systematically investigated. The results show that the phase composition of the as-prepared TiO_2 depends on medium pH value. The anatase proportion increases with pH value when pH < 3, whereas it decreases with pH when pH > 3. At pH = 3, the synthesised TiO_2 is pure anatase. Meanwhile, the reaction temperature does not affect the phase composition but the particle size. Higher reaction temperature results in larger particle size. The performance of DSSCs fabricated with the as-synthesised TiO_2 powders has a very close corresponding relation to the anatase fraction in TiO_2. The DSSC with the pure anatase TiO_2 synthesised at 140°C and under pH of 3 performs the best with a short-circuit current density of 8.17 mA/cm^2 and photo-to-electric energy conversion efficiency of 3.64%. The performance of all the TiO_2 prepared by hydrothermal synthesis is better than that of the commonly used commercial TiO_2 powder P25. Hydrothermal synthesis is highly recommended to be developed to produce nanocrystalline TiO_2 powder of high quality for DSSCs.

5. Acknowledgments: This work was partially supported by the National Science Foundation of China (NSFC, Grant No. 20976063). The authors express their gratitude to Xiaoming Fang and her student Lijuan Han for providing help in the performance measurement of DSSCs.

6 References

[1] Yella A., Lee H.W., Tsao H.N., *ET AL.*: 'Porphyrin-sensitized solar cells with cobalt (II/III)-based redox electrolyte exceed 12 percent efficiency', *Science*, 2011, **334**, pp. 629–633

[2] Nag M., Basak P., Manorama S.V.: 'Low-temperature hydrothermal synthesis of phase-pure rutile titania nanocrystals: time temperature tuning of morphology and photocatalytic activity', *Mater. Res. Bull.*, 2007, **42**, pp. 1691–1704
[3] Liao D.L., Liao B.Q.: 'Shape, size and photocatalytic activity control of TiO_2 nanoparticles with surfactants', *J. Photochem. Photobiol. A, Chem.*, 2007, **187**, pp. 363–369
[4] Wang W.J., Gu M.Y., Jin Y.P.: 'Effect of PVP on the photocatalytic behavior of TiO_2 under sunlight', *Mater. Lett.*, 2003, **57**, pp. 3276–3281
[5] Wang C.C., Ying J.Y.: 'Sol-gel synthesis and hydrothermal processing of anatase and rutile titania nanocrystals', *Chem. Mater.*, 1999, **11**, pp. 3113–3120
[6] Rao A.R., Dutta V.: 'Low-temperature synthesis of TiO_2 nanoparticles and preparation of TiO_2 thin films by spray deposition', *Sol. Energy Mater. Sol. Cells*, 2007, **91**, pp. 1075–1080
[7] Yang X.F., Konishi H., Xu H.F., Wu M.M.: 'Comparative Sol-hydro (solv-o)thermal synthesis of TiO_2 nanocrystals', *Eur. J. Inorg. Chem.*, 2006, **11**, pp. 2229–2235
[8] Wu L., Yu J.C., Wang X.C., Zhang L.Z., Yu J.G.: 'Characterization of mesoporous nanocrystalline TiO_2 photocatalysts synthesized via a sol-solvothermal process at a low temperature', *J. Solid State Chem.*, 2005, **178**, pp. 321–328
[9] Wahi R.K., Liu Y.P., Falkner J.C., Colvin V.L.: 'Solvothermal synthesis and characterization of anatase TiO_2 nanocrystals with ultrahigh surface area', *J. Colloid Interface Sci.*, 2006, **302**, pp. 530–536
[10] Byrappa K., Adschiri T.: 'Hydrothermal technology for nanotechnology', *Prog. Cryst. Growth Chem.*, 2007, **53**, pp. 117–166
[11] Wang G.H.: 'Hydrothermal synthesis and photocatalytic activity of nanocry-stalline TiO_2 powders in ethanol–water mixed solutions', *J. Mol. Catal. A, Chem.*, 2007, **274**, pp. 185–191
[12] Yan M.C., Chen F., Zhang J.L., Anpo M.: 'Preparation of controllable crystalline titania and study on the photocatalytic properties', *J. Phys. Chem. B*, 2005, **109**, pp. 8673–8678
[13] Zhou C.H., Xu S., Yang Y., *ET AL.*: 'Titanium dioxide sols synthesized by hydrothermal methods using tetrabutyl titanate as starting material and the application in dye sensitized solar cells', *Electrochim. Acta*, 2011, **56**, pp. 4308–4314
[14] Pavasupree S., Jitputti J., Ngamsinlapasathian S., Yoshikawa S.: 'Hydrothermal synthesis, characterization, photocatalytic activity and dye-sensitized solar cell performance of mesoporous anatase TiO_2 nanopowders', *Mater. Res. Bull.*, 2008, **43**, pp. 149–157
[15] Zhang Q.H., Gao L., Guo J.K.: 'Preparation and characterization of nanosized TiO_2 powders from aqueous $TiCl_4$ solution', *Nanostruct. Mater.*, 1999, **11**, pp. 1293–1300
[16] Zhang Q.H., Gao L., Guo J.K.: 'Effects of calcination on the photocatalytic properties of nanosized TiO_2 powders prepared by $TiCl_4$ hydrolysis', *Appl. Catal. B, Environ.*, 2000, **26**, pp. 207–215
[17] Yin H.B., Wada Y.J., Kitamura T., *ET AL.*: 'Hydrothermal synthesis of nanosized anatase and rutile TiO_2 using amorphous phase TiO_2', *J. Mater. Chem.*, 2001, **11**, pp. 1694–1703
[18] Yanagisawa K., Ovenstone J.: 'Crystallization of anatase from amorphous titania using the hydrothermal technique: effects of starting material and temperature', *J. Phys. Chem. B*, 1999, **103**, pp. 7781–7787
[19] Coronado D.R., Gattorno G.R., Pesqueira M.E.E., Cab C., de Coss R., Oskam G.: 'Phase-pure TiO_2 nanoparticles: anatase, brookite and rutile', *Nanotechnology*, 2008, **19**, p. 145605
[20] Bucsa R.R., Grätzel M.: 'Rutile formation in hydrothermally crystallized nanosized titania', *J. Am. Ceram. Soc.*, 1996, **79**, pp. 2185–2188
[21] Yang J., Mei S., Ferreira J.M.F.: 'Hydrothermal synthesis of nanosized titania powders: influence of peptization and peptizing agents on the crystalline phases and phase transitions', *J. Am. Ceram. Soc.*, 2000, **83**, pp. 1361–1368
[22] Zhang J., Zhang Y.P., Yu L.Q., Zhong X.L.: 'Preparation of nanotitania by hydrothermal method and progress in research of photocatalytic properties', *Inorg. Chem. Ind.*, 2010, **42**, pp. 6–9
[23] Yang J., Mei S., Ferreira J.M.F.: 'Hydrothermal synthesis of TiO_2 nanopowders from tetraalkylammonium hydroxide peptized sols', *Mater. Sci. Eng. C, Mater.*, 2001, **15**, pp. 183–185
[24] Grätzel M.: 'Demonstrating electron transfer and nanotechnology: a natural dye–sensitized nanocrystalline energy converter', *J. Chem. Educ.*, 1998, **75**, pp. 752–756
[25] Park N.G., van de Lagemaat J., Frank A.J.: 'Comparison of dye-sensitized rutile- and anatase-based TiO_2 solar cells', *J. Phys. Chem. B*, 2000, **104**, pp. 8989–8994
[26] Yu J.C., Zhang L.Z., Yu J.G.: 'Direct sonochemical preparation and characerization of highly active mesoporous TiO_2 with a bicrystalline framework', *Chem. Mater.*, 2002, **14**, pp. 4647–4653
[27] Zhang J.H., Xiao X., Nan J.M.: 'Hydrothermal-hydrolysis synthesis and photocatalytic properties of nano-TiO_2 with an adjustable crystalline structure', *J. Hazard. Mater.*, 2010, **176**, pp. 617–622
[28] Zhang H.Z., Banfield J.F.: 'Understanding polymorphic phase transformation behavior during growth of nanocrystalline aggregates: insights from TiO_2', *J. Phys. Chem. B*, 2000, **104**, pp. 3481–3487
[29] Fan K., Liu M., Peng T.Y., Ma L., Dai K.: 'Effects of paste components on the properties of screen-printed porous TiO_2 film for dye-sensitized solar cells', *Renew. Energy*, 2010, **35**, pp. 555–561
[30] Li M., Liu Y., Wang H., Shen H.: 'Synthesis of TiO_2 submicro-rings and their application in dye-sensitized solar cell', *Appl. Energy*, 2011, **88**, pp. 825–830

doi: 10.1049/mnl.2012.0941